

# Evaluation of the Ultrastructural and In Vitro Flow Properties of the PRESERFLO MicroShunt

Marta Ibarz Barberá<sup>1,2</sup>, Jose Luis Hernández-Verdejo<sup>3</sup>, Jean Bragard<sup>4</sup>,  
Javier Burguete<sup>4</sup>, Laura Morales Fernández<sup>5,6</sup>, Pedro Tañá Rivero<sup>7</sup>,  
Rosario Gómez de Liaño<sup>5</sup>, and Miguel A. Teus<sup>8-10</sup>

<sup>1</sup> Grupo Oftalvist, Madrid, Spain

<sup>2</sup> Hospital Moncloa, HLA Hospitales, Madrid, Spain

<sup>3</sup> Universidad Complutense de Madrid, Facultad de Óptica y Optometría

<sup>4</sup> Universidad de Navarra, Dept. of Physics and Applied Math

<sup>5</sup> Hospital Clínico, Madrid, Spain

<sup>6</sup> Hospital Quirón Pozuelo, Madrid, Spain

<sup>7</sup> Grupo Oftalvist, Alicante, Spain

<sup>8</sup> Clínica Novovisión, Madrid, Spain

<sup>9</sup> Hospital universitario "Príncipe de Asturias," Alcalá de Henares, Madrid, Spain

<sup>10</sup> Universidad de Alcalá, Alcalá de Henares, Madrid, Spain

**Correspondence:** Marta Ibarz Barberá, Avenida Isaac Albéniz 4E, Madrid 28224, Spain.  
E-mail: [marta@martaibarz.com](mailto:marta@martaibarz.com)

**Received:** August 24, 2021

**Accepted:** October 21, 2021

**Published:** November 18, 2021

**Keywords:** PRESERFLO; aqueous flow; pressure drop; glaucoma surgery; Hagen-Poiseuille

**Citation:** Barberá MI, Hernández-Verdejo JL, Bragard J, Burguete J, Fernández LM, Rivero PT, de Liaño RG, Teus MA. Evaluation of the ultrastructural and in vitro flow properties of the PRESERFLO microshunt. *Transl Vis Sci Technol.* 2021;10(13):26, <https://doi.org/10.1167/tvst.10.13.26>

**Purpose:** To measure the in vitro flow properties of the PRESERFLO implant for comparison with the theoretical resistance to flow.

**Methods:** The PRESERFLO was designed to control the flow of aqueous humor according to the Hagen-Poiseuille (HP) equation. Scanning electron microscopy (SEM) was performed to analyze the ultrastructure, and flow measurements were carried out using a gravity-flow setup.

**Results:** SEM images of the PRESERFLO showed luminal diameters of  $67.73 \times 65.95 \mu\text{m}$  and  $63.66 \times 70.54 \mu\text{m}$ . The total diameter was  $337.2 \mu\text{m}$ , and the wall was  $154 \mu\text{m}$  wide. The theoretical calculation of the resistance to flow (R) for an aqueous humor (AH) viscosity of 0.7185 centipoises (cP) was  $1.3 \text{ mm Hg}/(\mu\text{L}/\text{min})$ . Hence, assuming a constant AH flow of  $2 \mu\text{L}/\text{min}$ , the pressure differential across the device ( $\Delta P$ ) was estimated to be  $2.6 \text{ mm Hg}$ . The gravity-flow experiment allowed us to measure the experimental resistance to flow, which was  $R_E = 1.301 \text{ mm Hg}/(\mu\text{L}/\text{min})$ , in agreement with the theoretical resistance to flow R given by the HP equation.

**Conclusions:** The experimental and theoretical flow testing showed that the pressure drop across this device would not be large enough to avoid hypotony unless the resistance to outflow of the sub-Tenon space was sufficient to control the intraocular pressure in the early postoperative period.

**Translational Relevance:** The fluid properties of glaucoma subconjunctival drainage devices determine their specific bleb-forming capacity and ability to avoid hypotony and therefore their safety and efficacy profile.

## Introduction

One of the main challenges of glaucoma drainage device surgery is the control of aqueous humor outflow in the early postoperative phase to prevent hypotony. In the absence of a flow restrictor

method, the resistance offered by the tissues that surround the glaucoma tube plate cannot prevent hypotony until at least approximately six weeks after surgery.<sup>1</sup> In this period, there is a risk of severe hypotony, choroidal hemorrhage<sup>2</sup> and anterior chamber flattening, all of which are vision-threatening situations.

In 1969, Anthony Molteno was the first to introduce pioneering concepts regarding the need for a large surface area to disperse the aqueous humor (AH) and the advantage of draining the aqueous away from the limbus.<sup>3</sup> All the long-tube drainage devices currently available are based on the concept of the Molteno implant, which has a tube attached to a large explant placed 9 to 10 mm away from the limbus. The original Molteno implant (Molteno Ophthalmic Limited, Dunedin, New Zealand) has been modified over the years in two ways: the development of valved mechanisms and surgical maneuvers to improve the control of aqueous humor outflow to reduce hypotony, and the enlargement of the plate<sup>4,5</sup> to obtain lower postoperative intraocular pressure (IOP).

The Ahmed glaucoma valve (AGV; New World Medical, Rancho Cucamonga, CA, USA) was the first glaucoma drainage device with a flow resistor made of folded silicone membranes pretensioned by the plate, designed to open and close at a certain pressure level to prevent hypotony.<sup>6</sup> In 2008, Moss and Trope,<sup>7</sup> using a gravity-driven flow test, found that half of the AGV valves tested showed a closing pressure below 6 mm Hg. The Baerveldt implant (BGI; Abbott Medical Optics, Santa Ana, CA, USA) was introduced in 1990 without a flow restrictor.<sup>5</sup> The placement of temporary sutures around or within the lumen of the tube,<sup>8,9</sup> or a two-stage procedure were proposed to control the outflow. Despite these modifications, the rates of hypotony reported for both implants were similar (12% for the Molteno with the modified technique, 14% for the AGV<sup>10</sup>) and also clinically relevant, regarding the possible devastating consequences to the eye.

The search for adequate control of aqueous humor outflow continues today with the design of new implants based on the Hagen-Poiseuille formula for flow restriction. The resistance to flow ( $R$ ) and the pressure drop ( $\Delta p$ ) can be modified by means of the length and width of a tube according to the Hagen-Poiseuille equation, which governs the fluid properties of a cylindrical pipe for noncompressible Newtonian fluids.<sup>11</sup> The outflow resistance and therefore the pressure differential increase linearly in relation to the length of the tube and decrease to the fourth power of the lumen radius. Thus two new “miniaturized” tubes have been released, the XEN glaucoma implant (XEN-GGM; Allergan Plc, Parsippany, NJ, USA) and the PRESERFLO MicroShunt (Santen Pharmaceutical Co., Osaka, Japan). They are designed to be implanted either ab interno (XEN) or ab externo (PRESERFLO) to connect the anterior chamber with the subconjunctival space without a valved mechanism or a plate located at the end of the tube. They

differ in their length and luminal diameter and therefore in their theoretical resistance to flow and pressure drop, which should be higher for XEN 45 (6 mm long, 45  $\mu\text{m}$  internal diameter) than for the PRESERFLO (8.5 mm long, 70  $\mu\text{m}$  internal diameter). The XEN 45 implant has been reported to be able to maintain backpressure above hypotony (an experimental steady-state pressure of 8.9 mm Hg with a calculated value of 10.98 mm Hg),<sup>12</sup> whereas PRESERFLO has not yet been proven to do so. In a laboratory study performed by the manufacturer,<sup>13</sup> the authors explained that the luminal diameter had to be greater than the diameter of a sloughed endothelial cell (40–50  $\mu\text{m}$ ) and that the empirical data generated by rabbit studies from Arrieta et al.<sup>14</sup> helped to “fine-tune” the lumen diameter to 70  $\mu\text{m}$ . The authors hypothesized that the Poiseuille equation “breaks down” at small tube diameters in extremely hydrophobic materials such as poly(styrene-block-isobutylene-block-styrene) (SIBS), which is the material of the PRESERFLO.

To the best of our knowledge, the real flow through this implant, as well as its resistance to flow, and the pressure drop have not been reported. In the current study, we analyze the ultrastructure of PRESERFLO with scanning electron microscopy (SEM) to confirm that the luminal diameter is consistent with the specifications provided by the manufacturer. In addition, we calculate the theoretical resistance to flow and pressure differential for PRESERFLO, XEN 45, and other glaucoma implants using the de Hagen-Poiseuille equation, and finally we perform an experimental fluid-flow test using a gravity-flow setup at different simulated IOPs through the PRESERFLO. Thus the aim of this study is to evaluate the theoretical and experimental flow properties of the PRESERFLO implant.

## Methods

The two different samples of the PRESERFLO MicroShunt that were used for each of the analyses (SEM and flow studies) were provided directly by the manufacturer, they were brand new, without any previous surgical or experimental use. The manufacturer-provided dimensions of the device are as follows: total length: 8.5 mm; external diameter: 350  $\mu\text{m}$ ; internal diameter: 70  $\mu\text{m}$ ; and 1 mm<sup>2</sup> wings located 4.4 mm posterior to the beveled tip of the implant designed to avoid migration from the initial location [Figure 1](#). For the SEM analysis, the PRESERFLO MicroShunt was cut transversally with a 45° cataract blade.

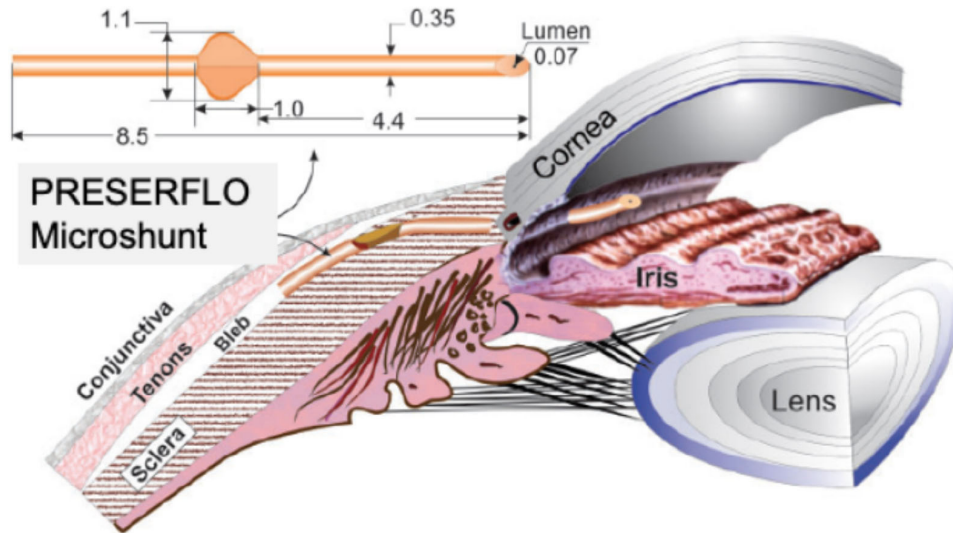


**Figure 1.** The PRESERFLO MicroShunt dimensions (mm) and location. The distal end is placed in the sub-Tenon space, and the proximal end is placed in the anterior chamber.

### Scanning Electron Microscope Analysis

The PRESERFLO luminal diameter was measured with a Quanta FEG 250 scanning electron microscope, which is a field-emission SEM (Fig. 2). Different measures were taken from the lumen, including edge to edge (vertically and horizontally), and edge to shadow. Measures from the lumen, wall, and total diameter are shown in Figure 3.

### Theoretical Calculation of the Resistance to Flow

The Hagen-Poiseuille equation<sup>11</sup> was used to calculate the theoretical resistance to flow ( $R$ , mm Hg/[ $\mu\text{L}/\text{min}$ ]) and the pressure differential or pressure drop ( $P = \Delta p = p_1 - p_2$ , mm Hg) through PRESERFLO for a known volumetric flow rate or AH production ( $Q$ ,  $\mu\text{L}/\text{min}$ ) and an AH viscosity of 0.7185 centipoises (cP) at 36°C for primary open-angle glaucoma.<sup>15</sup> In our flow experiments, we used the known dynamic viscosity of water  $\mu = 0.9775$  centipoises (cP) at 760 mmHg = 1 atm = 101325 Pa.s (SI) and  $T = 21^\circ\text{C}$ . Note that the dynamic viscosity of the AH is only 2% higher than the dynamic viscosity of water at the same temperature. We used the version of the Hagen-Poiseuille equation that accounts for the diameter ( $d^4$ ) and not the radius ( $r^4$ ). In this case, the proportionality constant number is 128 instead of 8:

$$P = Q \times R$$

$$P = \frac{128 \times \mu \times L \times Q}{\pi \times d^4}$$

$$R = \frac{128 \times \mu \times L}{\pi \times d^4}$$

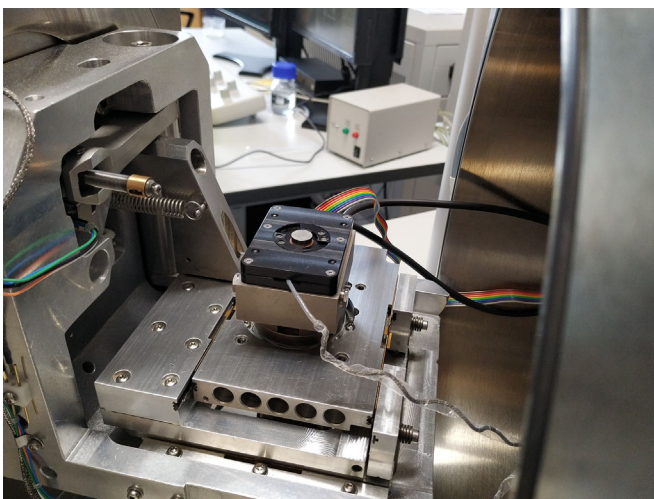


**Figure 2.** Image of the Quanta FEG 250 scanning electron microscope.



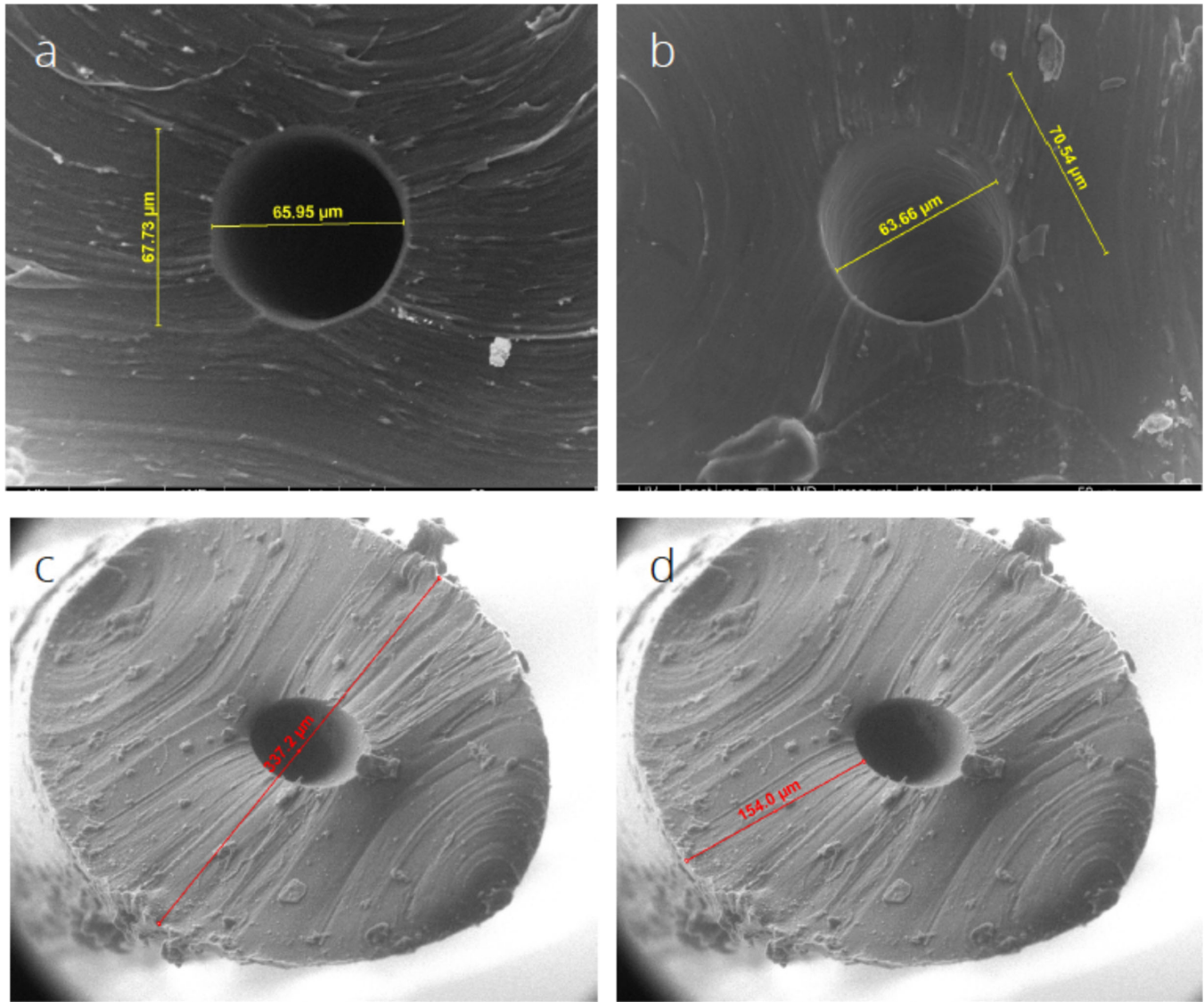


**Figure 3.** SEM images of the lumen diameter measured with the caliper tool. (a) Luminal diameter 67.73 × 65.95 μm. (b) Luminal diameter 63.66 × 70.54 μm. (c) Total diameter: 337.2 μm. (d) Wall: 154 μm.

$$P = \Delta p = p_1 - p_2 \text{ (pressure drop along the lumen of the tube)}$$

$\mu$  = dynamic viscosity

$L$  = length

$Q$  = volumetric flow rate

$R$  = resistance to flow

where  $R$  is the resistance to flow of the device, which is expressed in units of mm Hg/(μL/min). From the geometrical characteristics of the device and the dynamic viscosity of the fluid, we can compute the theoretical resistance to flow through the Hagen-Poiseuille flow.

## Flow Study

The experimental setup followed the main features of the experiment conducted by Estermann et al.<sup>16</sup> Figure 4 shows the overall experimental setup.

## Results

### SEM Analysis

The results from the measurements of two SEM images are shown in Figure 3.

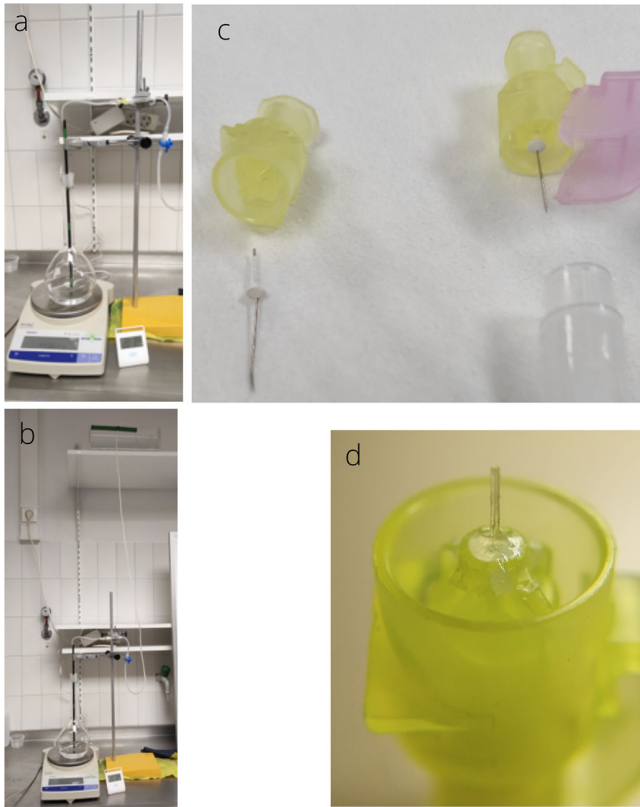


**Figure 4.** Experimental setup. The PRESERFLO is inserted into a tube with a large diameter ( $D_T = 1$  mm), with both ends immersed in a physiological saline solution of sodium chloride used to limit the presence of bubbles in the fluid circuit, connecting two different containers located at different heights. Once the fluid has crossed the implant, it continues through the tube until it reaches the bottom container. The difference in height between the top fluid reservoir and the bottom container induces the hydrostatic pressure  $P$ . This hydrostatic pressure is the only motor behind the fluid flow in the circuit according to the Hagen-Poiseuille law. No surface tension mechanisms (such as droplet formation) should affect the dynamics.

## Theoretical Calculation of the Resistance to Flow

The results from the theoretical calculation of  $R$  and  $P$  for each glaucoma implant are shown in [Figure 5](#).

## Experimental Flow Study

[Figure 6](#) shows the time evolution of the collected mass as a function of time. The volumetric flow measured was  $Q = 35.22$  ( $\mu\text{L}/\text{min}$ ) for a pressure  $P$  of  $58.92$  mm Hg. From the linear fit ( $R^2 = 0.9241$ ), the estimated resistance to flow was  $R_E = 1.806$  mm Hg/ $(\mu\text{L}/\text{min})$  with a computed confidence interval of 95% [ $1.571$ ;  $2.041$ ] mm Hg/ $(\mu\text{L}/\text{min})$ . To compare the results with the parameters present in a physiological environment, we estimated the resistance of the

PRESERFLO MicroShunt to be  $RE_{\text{PHYS}} = R_E \times (\mu_{\text{AQHUM}}/\mu_{\text{WATER}}) = 1.301$  mm Hg/ $(\mu\text{L}/\text{min})$ , in excellent agreement with the theoretical predicted value  $R = 1.3$  mm Hg/ $\mu\text{L}/\text{min}$ , and the pressure drop was estimated to be  $2.6$  mm Hg.

With the estimated Reynolds number for the present fluid experiment for a flow of  $60$   $\mu\text{L}/\text{min}$  and an average speed of approximately  $0.26$  (m/s), our experiment operated for Reynolds numbers in the range between  $25$  and  $60$ , far below the transition to the turbulent regime. This meant that even for such a high applied pressure, the flow was still laminar, and the Hagen-Poiseuille law was still valid.

## Discussion

In recent years, advancements in glaucoma tube development for flow restriction have brought new implants to the glaucoma surgery spectrum that aim not only to prevent hypotony but also to simplify and standardize the surgical technique, with the goal of a lower rate of postoperative complications. The objective is twofold: to reach sufficient flow restriction to decrease the risk of hypotony without undermining the drainage efficacy and to maintain the lowest possible IOP once a filtering bleb has been developed.

Sheybani et al.,<sup>12</sup> in an experimental flow test of the XEN 45, showed that the implant was capable of maintaining the backpressure above numerical hypotony (defined as an IOP  $\leq 5$  mm Hg, after surgery by the World Glaucoma Association Guidelines<sup>19</sup>). The experimental steady-state pressure reported for XEN 45 by the authors was  $8.9$  mm Hg, and the resistance to flow was  $4.393$  mm Hg/ $(\mu\text{L}/\text{min})$ ,  $3.4$ -fold higher than the experimental resistance to flow ( $R_E = 1.301$  mm Hg/ $\mu\text{L}/\text{min}$ ) and pressure drop ( $2.6$  mm Hg) measured for the PRESERFLO with our experimental setup, suggesting that PRESERFLO would not be able to avoid hypotony ( $5$  mm Hg) just by means of its flow restriction properties. Given that the clinical rates of hypotony reported for PRESERFLO in the literature are much lower than expected by the results of the laboratory tests, it is reasonable to believe that there must be crucial control of the outflow exerted initially by the Tenon capsule and later by the remodeling of the subconjunctival tissue.

In a study published by Scheres et al.,<sup>20</sup> the incidences of hypotony with the PRESERFLO and the XEN 45 were comparable. In fact, they found that during the first week after surgery, although the rate of hypotony was higher with PRESERFLO ( $39\%$ ) than with XEN 45 ( $24\%$ ), the need for anterior chamber reformation was lower ( $2\%$  PRESERFLO,  $5\%$  XEN

**PRESERFLO Microshunt:**

$$R = \frac{128 \times 0.7185 \times 1.25 \times 10^{-7} \times 8.5}{3.1416 \times 0.07^4}$$

$$R = 1.3 \text{ mmHg}/\mu\text{L}/\text{min}$$

$$P = 2 \times 1.3$$

$$P = 2.6 \text{ mmHg}$$

**Ex-Press P-200:**

$$R = \frac{128 \times 0.7185 \times 1.25 \times 10^{-7} \times 2.56}{3.1416 \times 0.377^4}$$

$$R = 0.0004 \text{ mmHg}/\mu\text{L}/\text{min}$$

$$P = 2 \times 0.0004$$

$$P = 0.0008 \text{ mmHg}$$

**Paul Glaucoma Implant:**

$$R = \frac{128 \times 0.7185 \times 1.25 \times 10^{-7} \times 10}{3.1416 \times 0.127^4}$$

$$R = 0.14 \text{ mmHg}/\mu\text{L}/\text{min}$$

$$P = 2 \times 0.14$$

$$P = 0.28 \text{ mmHg}$$

**XEN 45:**

$$R = \frac{128 \times 0.7185 \times 1.25 \times 10^{-7} \times 6}{3.1416 \times 0.045^4}$$

$$R = 5.35 \text{ mmHg}/\mu\text{L}/\text{min}$$

$$P = 2 \times 5.35$$

$$P = 10.7 \text{ mmHg}$$

**Ahmed AGV, Baerveldt BGI, Molteno:**

$$R = \frac{128 \times 0.7185 \times 1.25 \times 10^{-7} \times 10}{3.1416 \times 0.305^4}$$

$$R = 0.004 \text{ mmHg}/\mu\text{L}/\text{min}$$

$$P = 2 \times 0.004$$

$$P = 0.008 \text{ mmHg}$$

**Figure 5.** According to the different internal diameters and lengths of each glaucoma drainage device (PRESERFLO MicroShunt, 70 μm, 8.5 mm; XEN45, 45 μm, 6 mm; Ahmed AGV, Baerveldt BGI, and Molteno 305 μm, 10 mm; Paul glaucoma implant, 127 μm, 10 mm), we calculated R and P for an aqueous humor flow rate of 2 μL/min (the aqueous humor flow rate has been reported to be 2.75 ± 0.63 μL/min [a range of 1.8 to 4.3 μL/min]<sup>17</sup>). For the Ex-PRESS implant (Alcon Laboratories, Inc., Fort Worth, TX, USA), the theoretical calculations of flow were performed only for the P200 model (377 μm, 2.56 mm) and not for the P50, which is more commonly used in clinical practice, because the P50 model has a 150 μm diameter bar placed across its lumen,<sup>18</sup> with implications on the fluid properties that prevent the theoretical calculation of the resistance to flow.

45), with the same rate of choroidal detachment for both implants (2%). In addition, after PRESERFLO implantation, Schlenker et al.<sup>21</sup> reported three out of 181 cases of anterior chamber reformation and four out of 181 cases of late choroidal detachment, and Batlle et al.<sup>22</sup> reported 13% shallow anterior chambers and 8.7% choroidal detachments during the first three weeks. In a previous study by our group,<sup>23</sup> we reported an 11% rate of hypotony.

Regarding trabeculectomy, Abbas et al.<sup>24</sup> reported a hypotony rate of 47% at any time during follow-up and 11% of persistent hypotony in two consecutive follow-up visits. In the Tube Versus Trabeculectomy study,<sup>25</sup>

the rate of persistent hypotony after trabeculectomy was 23% at three years, increasing to 31% at 5 years.

The Ahmed versus Baerveldt study<sup>10</sup> reported a similar rate of hypotony after one year of follow-up (14%) for both implants. The AGV and the Baerveldt implants share the same resistance to flow (R = 0.004 mm Hg/μL/min) but differ in the pressure drop across the tube (0.008 mm Hg for Baerveldt, 13.6 mm Hg, and 6.1 mm Hg opening and closing pressures for AGV<sup>6</sup>) because of the valved mechanism of the AGV. In vitro testing of the AGV model FP7 showed significant variability in the closing pressure, with half closing at IOPs considered potentially problematic in clinical



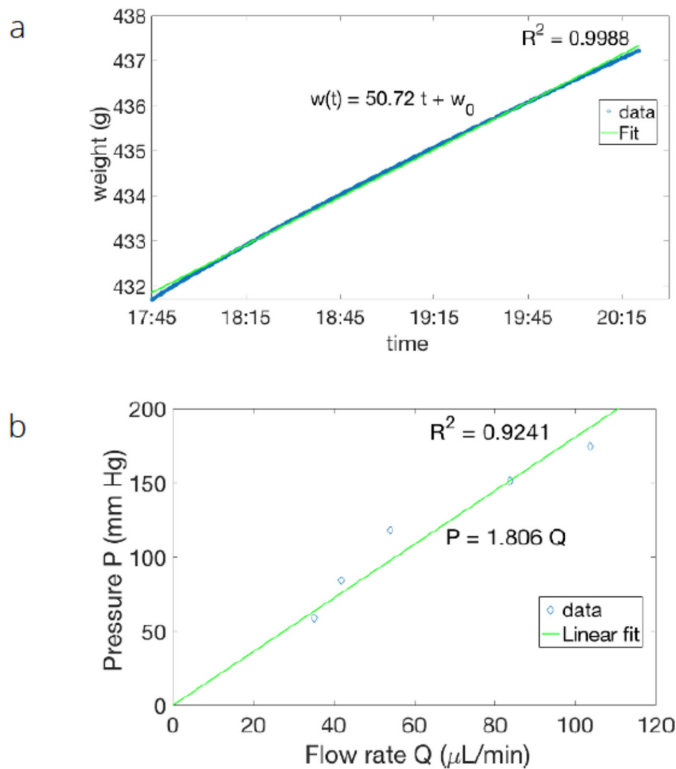


**Figure 6.** Time evolution of the collected mass as a function of time. (a) Results obtained by moving the upper fluid reservoir and therefore modifying the applied pressure  $P$ . According to the Hagen-Poiseuille law, a constant applied pressure difference induces a constant flow, the flow is measured in terms of the collected mass, and the linear growth of the mass as a function of time allows us to determine the flow. The initial difference in height between the top container and the bottom container was 80.1 cm. Assuming that the physiological solution used in our experiment had the same density as water, it was converted into a pressure difference of  $P = 58.92$  mm Hg. The linear fit ( $R^2 = 0.9988$ ) of the collected data was approximated by  $w(t) = 50.72 t + w_0$ , where  $w(t)$  is the weight in grams and  $t$  is the time expressed in a fraction of the 24-hour period. For the fixed pressure, the observed mass flow was given by  $Q = 50.72$  g/(24 h) with a 95% confidence interval of [50.71; 50.74] g/(24 h). The linear fit was excellent; indeed, the confidence interval for the estimated mass flow was very narrow and only affected the fourth significant digit. The volumetric flow was also expressed in more conventional units as  $Q = 35.22$  ( $\mu\text{L}/\text{min}$ ) for a pressure  $P$  of 58.92 mm Hg. (b) At five different heights, the flow rate ( $Q$ ) was expressed as a function of the applied pressure ( $P$ ) through a linear fit ( $R^2 = 0.9241$ ). From the data, the resistance to flow was estimated to be  $R_E = 1.806$  mm Hg/( $\mu\text{L}/\text{min}$ ) with a computed confidence interval at 95% of (1.571; 2.041) mm Hg/( $\mu\text{L}/\text{min}$ ). Note that error bars are not shown on the data because they are very small (less than the diamond symbol size).

situations (1.4, 3.2, 3.5 mm Hg).<sup>7</sup> The FP7 AGV is made of silicone, which is much less stiff than the previous polypropylene, and may probably have a less precise opening pressure.<sup>7</sup>

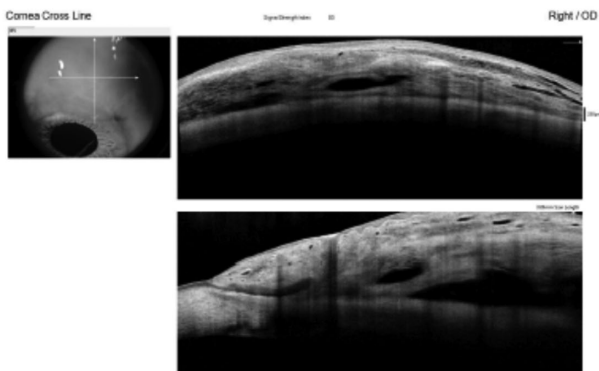
Compared to the new short tubes (XEN 45, PRESERFLO), only a randomized control trial that included a significant number of patients would show

the real clinical differences between them, but the clinical results reported so far suggest that the rates of hypotony expected for them are not higher than those reported for the long-tube drainage devices. The Paul glaucoma implant<sup>26</sup> is an example of the progressive tendency to narrow the luminal diameter of the tube to search for the ideal size to control the outflow in long tubes. This implant does not have a valved mechanism to restrict the flow of aqueous. According to the Hagen-Poiseuille equation, the theoretical pressure drop of this implant would be 0.28 mm Hg, far below 5 mm Hg. Nevertheless the hypotony rates reported are quite similar to those of the Ahmed and Baerveldt drainage devices (14.9% rate of self-limiting shallow anterior chamber and 9.5% hypotony requiring intervention).<sup>27</sup>

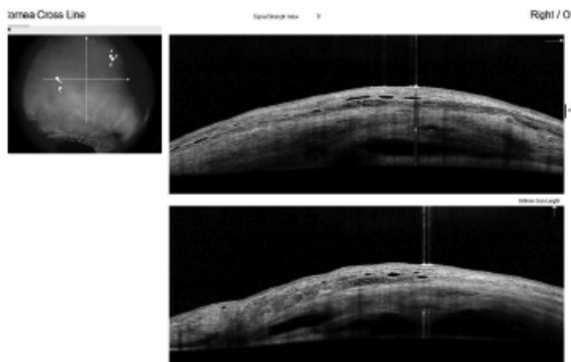
The tissue response to the flow rate of aqueous humor and the formation of a characteristic type of filtering bleb could explain the low incidence of hypotony reported for the PRESERFLO implant. In a study published by our group,<sup>23</sup> we analyzed the morphology and geometry of the blebs formed after the implantation of PRESERFLO with anterior segment optical coherence tomography (AS-OCT). From the early postoperative period to the third month, the aqueous humor displaces the tissues to form fluid cavities underneath the Tenon, that showed a measurable horizontal and vertical expansion and a multilayered appearance of the overlying conjunctival stroma in the majority of the cases. The morphology of the blebs in the early postoperative period resembled that of classic trabeculectomy blebs. A longer follow-up of the same patients up to one year showed that the bleb maturation process led to the formation of thick hypo reflective walls, as happened in the maturation process after trabeculectomy (Fig. 7). In contrast, the AS-OCT morphology of the filtering blebs associated with XEN has been described as low-lying, diffuse,<sup>28</sup> or a “filtering conjunctiva,”<sup>27</sup> without a conventional bleb, suggesting that the lower flow through the XEN vs the PRESERFLO probably accelerates the subconjunctival fibrotic response, thus increasing the number of needlings required (43%–71% XEN vs. 8.5% PRESERFLO<sup>21</sup>). The location of the distal end of the implant and the surgical technique (“ab interno” vs. “ab externo”) may also determine the ability of a tube to form functioning filtering blebs. Lenzofer et al.<sup>29</sup> showed with AS-OCT that the XEN gel stents located in deeper locations (the Tenon layer above the outer stent lumen) achieved higher IOP reductions and lower secondary needling rates (68% sub-Tenon, 80% intraconjunctival). The “ab interno” technique used to implant the XEN device has been reported to be less prone to bleb formation because of a higher resistance to flow of the tissues.<sup>30</sup> Most likely,

## Hyporeflective bleb wall and discrete fluid cavity

6 months



6 months



1 year

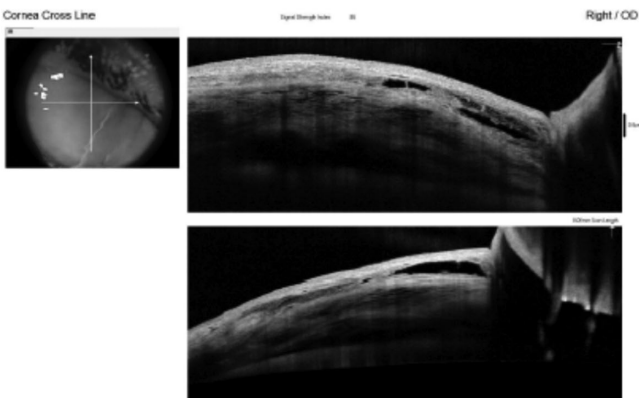


**Figure 7.** AS-OCT image of the hyporeflective bleb wall and discrete fluid cavity of a PRESERFLO bleb. Evolution from six months to one year.

the “ab interno” approach makes it difficult to identify the layers of the conjunctiva-Tenon complex to place the tip of the implant underneath the Tenon capsule. One of the key aspects of PRESERFLO is the “ab externo” dissection of the virtual space located between the conjunctiva and the Tenon capsule<sup>31</sup> to create a wide pocket where the bleb forming process initiates. Narita et al.<sup>32</sup> suggested the necessity to leave the Tenon capsule as it is during trabeculectomy to facilitate the formation of thick and hypo reflective bleb walls, the same principle followed during the surgical technique used to implant a PRESERFLO. Maintaining the anatomy of the Tenon capsule seems to be an important factor in controlling the outflow in the early postoperative period with this device. The sequence of AH outflow control by the subconjunctival tissue response might well be as follows: the mere presence of the fluid,<sup>33</sup> as well as the presence of inflamma-

tory mediators (cytokines) in the AH of primary open-angle glaucoma patients<sup>34</sup> that initiates the fibrovascular response of the tissues to form the filtering bleb that ultimately modulates AH absorption, takes a few weeks to occur.<sup>1</sup> In the very early postoperative period when the fibrovascular response has not yet been initiated, the resistance to flow offered by the Tenon capsule against the amount of AH delivered by the implant (directly proportional to the preoperative intraocular pressure but restricted by its length and diameter) might be the main factor involved in the prevention of hypotony.

When the AH is released in the sub-Tenon space at a certain flow rate, lower than the capillary pressure of the surrounding tissues, a fibrovascular response is initiated at the capsule toward the formation of a bleb wall,<sup>1</sup> whose porosity and therefore hydraulic conductivity are sufficient to maintain a



constant flow of AH from the anterior chamber, tube, bleb wall and finally the episcleral venous system. According to a study published by Gardiner et al.,<sup>35</sup> the diameter of the tube becomes irrelevant when the pressure between the anterior chamber and the bleb reaches equilibrium. Lim<sup>6</sup> dissents somehow from Gardiner's et al. hypothesis, advocating that neither the XEN 45 nor the PRESERFLO address the problem of "resistor in series," meaning that once bleb resistance has occurred, the flow restrictor within the tube actually becomes redundant and even detrimental to achieving the lowest possible IOP.

Based on the outcomes of the current experiment, which operates at Reynolds numbers in the range of 25 to 60 (far below the transition to the turbulent regime), even for such a high applied pressure, the flow is still laminar, and the Hagen-Poiseuille law is still valid for measuring the resistance to flow through the PRESERFLO MicroShunt.

In conclusion, despite the theoretical and experimental inability of the PRESERFLO MicroShunt to protect against hypotony, the clinical results reported suggest that the tissue response to the particular flow rate of the aqueous humor provided by this implant provides enough resistance to flow to maintain the intraocular pressure above hypotony in most cases.

## Acknowledgments

The authors thank the Department of Physics and Applied Math of the University of Navarra and the Laboratory of Advanced Microscopy of the University of Zaragoza for their non-profit contribution to the overall investigation and manuscript.

Disclosure: **M.I. Barberá**, None; **J.L. Hernández-Verdejo**, None; **J. Bragard**, None; **J. Burguete**, None; **L.M. Fernández**, None; **P.T. Rivero**, None; **R.G. de Liaño**, None; **M.A. Teus**, None

## References

1. Molteno A, Fucik M, Dempster A, Bevin T. Otago glaucoma surgery study. Factors controlling capsule fibrosis around Molteno implants with histopathological correlation. *Ophthalmology*. 2003;110:2198–2206.
2. Gressel MG, Parrish RK, Heuer DK. Delayed non-expulsive suprachoroidal haemorrhage. *Arch Ophthalmol*. 1984;102:1757–1760.
3. Molteno ACB, Dempster AG, Carne A. Molteno implants: the principles of bleb management. *Aust N Z J Ophthalmol*. 1999;27:350–352.
4. Britt MT, LaBree LD, Lloyd MA, et al. Randomized clinical trial of the 350-mm<sup>2</sup> versus the 500-mm<sup>2</sup> Baerveldt implant: longer term results: is bigger better? *Ophthalmology*. 1999;106:2312–2318.
5. Lloyd MA, Baerveldt G, Heuer DK, et al. The Baerveldt glaucoma implant-long term histologic studies in rabbits and clinical experience in humans. *Invest Ophthalmol Vis Sci*. 1991;32:746–746.
6. Lim KS. Control and optimisation of fluid flow in glaucoma drainage device surgery. *Eye (Lond)*. 2018;32:230–234.
7. Moss EB, Trope GE. Assessment of closing pressure in silicone Ahmed FP7 glaucoma valves. *J Glaucoma*. 2008;17:489–493.
8. Egbert PR, Lieberman MF. Internal suture occlusion of the Molteno glaucoma implant for the prevention of postoperative hypotony. *Ophthalmic Surg*. 1989;20:53–56.
9. El-Sayyad F, el-Maghraby A, Helal M, et al. The use of releasable sutures in Molteno glaucoma implant procedures to reduce postoperative hypotony. *Ophthalmic Surg*. 1991;22:82–84.
10. Christakis PG, Jeffrey W, Kalena JW, et al. The Ahmed Versus Baerveldt Study. *Ophthalmology*. 2011;118:2180–2189.
11. McEwen W. Application of Poiseuille's law to aqueous outflow. *Arch Ophthalmol*. 1958;60:290–294.
12. Sheybani A, Reitsamer H, Ahmed II. Fluid dynamics of a novel micro-fistula implant for the surgical treatment of glaucoma. *Invest Ophthalmol Vis Sci*. 2015;56:4789–4795.
13. Pinchuk L, Riss I, Battle JF, et al. The development of a micro-shunt made from poly(styrene-block-isobutylene-block-styrene) to treat glaucoma. *J Biomed Mater Res B Appl Biomater*. 2017;105:211–221.
14. Arrieta EA, Aly M, Parrish R, Dubovy S. Clinicopathologic correlations of poly-(styrene-bisobutylene-b-styrene) glaucoma drainage devices of different internal diameters in rabbits. *Ophthalmic Surg Lasers Imaging*. 2011;42:338–345.
15. Vass C, Hirn C, Unger E, et al. Human aqueous humor viscosity in cataract, primary open angle glaucoma and pseudoexfoliation syndrome. *Invest Ophthalmol Vis Sci*. 2004;45:5030.
16. Estermann S, Yuttitham K, Chen JA, Lee OT, Stamper RL. Comparative in vitro flow study of 3 different Ex-PRESS miniature glaucoma device models. *J Glaucoma*. 2013;22:209–214.

17. Brubaker RF. Flow of aqueous humor in humans. *Invest Ophthalmol Vis Sci.* 1991;32:3145–3167.
18. Samsudin A, Eames I, brocchini S, Tee Kaw P. Evaluation of dimensional and flow properties of ExPress glaucoma drainage devices. *J Glaucoma.* 2016;25:e39–e45.
19. Shaaraway T, Sherood M, Grehn F. *WGA Guidelines on design and reporting of glaucoma surgical trials.* Amsterdam, The Netherlands: Kugler Publications; 2009.
20. Scheres LMJ, Kujovic-Aleksov S, Ramdas WD, et al. XEN Gel Stent compared to PRESERFLO MicroShunt implantation for primary open-angle glaucoma: two-year results. *Acta Ophthalmol.* 2021;99(3):e433–e440.
21. Schlenker MB, Durr GM, Michaelov E, Ahmed IIK. Intermediate outcomes of a novel standalone Ab Externo SIBS Microshunt with mitomycin C. *Am J Ophthalmol.* 2020;215:141–153.
22. Battle JF, Fantes F, Riss I, et al. Three-year follow-up of a novel aqueous humor MicroShunt. *J Glaucoma.* 2016;25(2):e58–65.
23. Ibarz Barberá M, Morales Fernández L, Tañá Rivero P, Gómez de Liaño R, Teus MA. Anterior-segment optical coherence tomography of filtering blebs in the early postoperative period of ab externo SIBS microshunt implantation with mitomycin C: Morphological analysis and correlation with intraocular pressure reduction [published online ahead of print April 10, 2021]. *Acta Ophthalmol.* <https://doi.org/10.1111/aos.14863>.
24. Abbas A, Agrawal P, King AJ. Exploring literature-based definitions of hypotony following glaucoma filtration surgery and the impact on clinical outcomes. *Acta Ophthalmol.* 2018;96:e285–e289.
25. Gedde SJ, Schiffman JC, Feuer WJ, Herndon LW, Brandt JD, Budenz DL; Tube versus Trabeculectomy Study Group. Treatment outcomes in the Tube Versus Trabeculectomy (TVT) study after five years of follow-up. *Am J Ophthalmol.* 2012;153:789–803.e2.
26. Koh V, Chew P, Triolo G, Lim KS, Barton K, Glaucoma Implant Study Group PAUL. Treatment outcomes using the PAUL glaucoma implant to control intraocular pressure in eyes with refractory glaucoma. *Ophthalmol Glaucoma.* 2020;3:350–359.
27. Teus MA, Moreno-Arrones JP, et al. Optical coherence tomography analysis of filtering blebs after long-term, functioning trabeculectomy and XEN stent implant. *Graefes Arch Clin Exp Ophthalmol.* 2019;257:1005–1011.
28. Lenzhofer M, Strohmaier C, Hohensinn M, et al. Longitudinal bleb morphology in anterior segment OCT after minimally invasive transscleral ab interno Glaucoma Gel Microstent implantation. *Acta Ophthalmol.* 2019;97(2):e231–e237.
29. Lenzhofer M, Strohmaier C, Sperl P, et al. Effect of the outer stent position on efficacy after minimally invasive transscleral glaucoma gel stent implantation. *Acta Ophthalmol.* 2019;97(8):e1105–e1111.
30. Lee R, Bouremel Y, Eames I, Brocchini S, Khaw P. The implications of an Ab interno versus ab externo surgical approach on outflow resistance of a subconjunctival drainage device for intraocular pressure control. *Transl Vis Sci Technol.* 2019;8:1–7.
31. Kozdon K, Caridi B, Duru I, Ezra DG, Phillips JB, Bailly M. A Tenon's capsule/bulbar conjunctiva interface biomimetic to model fibrosis and local drug delivery. *PLoS One.* 2020;15(11):e0241569.
32. Narita A, Morizane Y, Miyake T, Seguchi J, Baba T, Shiraga F. Characteristics of successful filtering blebs at 1 year after trabeculectomy using swept-source three-dimensional anterior segment optical coherence tomography. *Jpn J Ophthalmol.* 2017;61:253–259.
33. Pandav SS, Ross CM, Thattaruthody F, et al. Porosity of bleb capsule declines rapidly with fluid challenge. *J Curr Glaucoma Pract.* 2016;10:91–96.
34. Freedman J. Tube-shunt bleb pathophysiology, the cytokine story. *J Glaucoma.* 2021;30:109–113.
35. Gardiner BS, Smith DW, Coote M, Crowston JG. Computational modeling of fluid flow and intraocular pressure following glaucoma surgery. *PLoS One.* 2010;5(10):1–11.